NASA TECHNICAL MEMORANDUM

NASA TM-78913

NASA TM-78913

FRACTOGRAPHIC EVALUATION OF CREEP EFFECTS ON STRAIN-CONTROLLED FATIGUE-CRACKING OF AISI 304LC AND 316 STAINLESS STEEL

by Robert E. Oldrieve
Lewis Research Center
Cleveland, Ohio 44135

June 1978

FRACTOGRAPHIC EVALUATION OF CREEP EFFECTS ON STRAIN-CONTROLLED FATIGUE-CRACKING OF AISI 304LC AND 316 STAINLESS STEEL

by Robert E. Oldrieve

NASA-Lewis Research Center

SUMMARY

An investigation was conducted in which fractography was used to characterize High-Temperature Low-Cycle (HTLC) creep-fatigue cracking of AISI 304LC and AISI 316 stainless steel specimens for each of four basic inelastic strainrange versus life relationships obtained by the method of Strainrange Partitioning (SRP). Previously, it has been suggested that differing deformation mechanisms were the cause of separation in the SRP relationships. Accordingly, this investigation was made to identify fracture features which can provide an understanding of the mechanisms which are operative in creep-fatigue.

Evaluation of the fractures and of crack initiation data obtained from the fractures show that each of the four types of SRP-cycles can be characterized as to the effect upon cracking of tensile, compressive, or the absence of creep-strain.

The fatigue fracture resulting from the non-creep-containing PP-cycle is transgranular from one or more surface-crack-initiation sites. It was determined that the introduction of creep strain (in the PC, CC, or CP-type cycles) acts to change fatigue fracture in three distinct ways:

(1) The number of surface transgranular crack-initiation sites (PC-cycle) is increased as compared to the non-creep fatigue (PP-cycle), resulting in fewer cycles in the crack initiation stage, a broad crack front, and shorter total cyclic life.

(2) Introduction of grain-boundary cracking at the crack front (CC-cycle) produces early crack initiation and transgranular-intergranular crack propagation (mixed fracture mode), resulting in shorter total life than for either the PP or PC cycle.

(3) Introduction of grain-boundary crack-initiation sites throughout the volume of the test specimen (CP-cycle) produces a total intergranular fracture. For this CP-cycle the total fatigue life (crack initiation plus propagation) was less than the crack initiation life for any of the other SRP-fatigue cycles for the same inelastic strainrange.

E-9648

INTRODUCTION

Analysis of High Temperature Low Cycle (HTLC) fatigue life data for AISI 304LC and 316 stainless steels results in four separate relationships between inelastic strainrange and cyclic life when creep strain, plastic strain, and loading direction are treated as they are in the method of Strainrange Partitioning (SRP, ref. 1). That the four plots, sometimes coincident or intersecting, may be determined by deformation mechanisms was suggested by the discussion of active slip and grain boundary sliding systems of reference 2. In effect, it is suggested that each SRP plot is a material property plot. If this is the case then the type of fracture, the time for cracks to initiate, or the rate of cracking may differ accordingly. This investigation,

therefore, was undertaken to identify by fractography specific crack propagation features which predominate in causing fracture for each type of SRP-cycle. A test cycle containing no creep strain is identified as a PP-cycle. When creep strain is applied in compression only, the test cycle is designated PC; when creep strain is applied in tension only, the test cycle is designated CP; and when creep strain is applied in both tension and compression the test cycle is designated CC.

As a means of identifying creep-effects, measurements were made of the crack propagation portion of total life as indicated by fracture surface markings. Crack initiation is defined as the cycles required to produce a crack depth of 125 μm (0.005 in.). The crack propagation portion of total life is equal to the number of cycles required to propagate this initiation depth crack to fracture of the specimen. For transgranular fracture, the crack propagation period was measured from the cyclic advance of the crack-front, as identified by striations (refs. 3 and 4), and for intergranular fracture by other features in the absence of striations. By these means crack initiation life, fracture mode, and surface features were related to the type of SRP test cycle and to total cyclic life.

Only a limited amount of investigative effort has been directed toward obtaining the effect of creep upon the fracture appearance of applied cyclic loads. For example, it has been shown that intergranular fatigue fracture can occur in alloys in the presence of creep strain whereas fracture would be transgranular in the absence of creep ((Co-base alloy L605 and Fe-base A286 (ref. 5)). A more unusual finding has been made for several materials which fail transgranularly when the fatigue cycle contains compressive creep only but fail intergranularly for otherwise identical test conditions except that the fatigue cycle contains tensile creep only, ((AISI 316 stainless steel (ref. 1) and Ta alloy T111 (ref. 6)). From these limited data, the factors that can contribute to a change in fatigue fracture mode and cyclic lifetime may be inferred as being the result not only of the amount of creep, but also by the direction of loading (tension or compression) which causes creep. The austenitic stainless steels were selected for a more complete investigation of this behavior.

The present investigation uses fractography to determine fracture mode, crack initiation period, and crack propagation rate for all four types of SRP-cycles. The conditions considered were selected so as to include a range of temperatures (305°C to 705°C), a range of inelastic strainranges (0.4% to 4%), and load application conditions in which creep-strain or plastic-strain predominated in tension or compress. . or both.

Descriptions of the test specimens, the methods of testing, specimen examination, crack propagation, fracture characteristics, and the observed features associated with each type of SRP cycle are presented in the sections which follow.

NOMENCLATURE

c	crack length (depth from surface)
C_i	crack initiation depth (125 μm)
c/2	crack half-length, μm
dc/dn	crack propagation rate, μm/cycle
$\Delta\varepsilon_i$	applied inelastic strainrange = $\Delta\varepsilon_{pp} + \Delta\varepsilon_{pc} + \Delta\varepsilon_{cc} + \Delta\varepsilon_{cp}$
$\Delta\varepsilon$	inelastic strainrange, specified as follows:
$\Delta\varepsilon_{pp}$	tensile plastic strain balanced by compressive plastic strain
$\Delta\varepsilon_{pc}$	tensile plastic strain balanced by compressive creep strain
$\Delta\varepsilon_{cc}$	tensile creep strain balanced by compressive creep strain
$\Delta\varepsilon_{cp}$	tensile creep strain balanced by compressive plastic strain
SEM	scanning electron microscopy
SRP	strainrange partitioning, with SRP-cycle as follows:
PP or PP-cycle	fatigue cycle consisting largely of $\Delta\varepsilon_{pp}$
PC or PC-cycle	fatigue cycle consisting largely of $\Delta\varepsilon_{pc}$
CC or CC-cycle	fatigue cycle consisting largely of $\Delta\varepsilon_{cc}$
CP or CP-cycle	fatigue cycle consisting largely of $\Delta\varepsilon_{cp}$
n	cycle
N_f	cycles to fail
ΔT	change in wall thickness by necking

MATERIALS AND EXPERIMENTAL DETAILS

Materials for which response to creep-fatigue cycling has been previously analyzed (ref. 1), were used in this investigation. They were Types AISI 304LC (low carbon) and 316 stainless steel. The nominal

compositions are: AISI 304LC (0.02 C, 1.5 Mn, 0.5 Si, 10 Ni, 19 Cr) and AISI 316 (0.08 C, 1.5 Mn, 0.5 Si, 12 Ni, 17 Cr, 2.5 Mo). Specimens of both alloys were tested in the fully annealed condition. Strainrange versus cyclic life relationships are reported for 316 steel in reference 7. Some of the data for 304LC are shown in reference 1.

The test specimens were of the tubular, hour-glass configuration with a nominal wall thickness of 1.53 mm, (0.060 in.). Heating was either by direct resistance or by internally positioned silicon carbide heating element. All tests were conducted using closed-loop, servo-controlled, electro-hydraulic equipment. Strains were measured using a diametral extensometer. All strains reported are longitudinal strains calculated from measured diametral strains. Further details of experimental procedures and test equipment can be found in reference 8. The four basic types of SRP cycles are designated PP, PC, CP, and CC-cycles. The letters P (plastic, time independent) and C (creep, time dependent) are used to designate the major types of inelastic strain. The first letter indicates the tensile and the second letter the compression portion of each applied cycle. In some cases the tensile deformation was applied at one temperature and the compression deformation at another. This is identified in table I.

The analytical technique of partitioning establishes a data correlation line for each of the four basic types of loading cycles. Test specimens selected for this study represent data points of very close proximity to the final PP, CC, PC, and CP lines which were determined analytically from the test data. The procedure for partitioning the cycles into SRP cycle components and the method by which the SRP-cycle plots were obtained is given in reference 7. The test conditions of the specimens used in the fractographic investigation described herein are given in table I in the order in which they appear in the figures. The selected test specimens were examined using scanning electron microscopy (SEM) to determine fracture characteristics and to measure crack propagation rates. Crack propagation rates were determined from the measurements of the spacing between striations formed as the crack front advanced assuming one striation per cycle. Macroscopic examination was used to supplement the SEM.

The number of cycles required for a crack to initiate to a depth of 125 μm (0.005 in.) was derived as follows: The number of cycles expended in crack propagation was determined by counting striations from specimen failure backwards to the initiation depth. Crack initiation was thus taken to be the difference between total cycles to failure and the number of counted striations.

CORRELATION OF FRACTURE APPEARANCE WITH STRAINRANGE CYCLE.

A general finding of this investigation is that creep-fatigue interaction results in a distinctive fracture appearance for each of four types of SRP test cycles. Figures 1 to 4 show fracture surfaces of AISI 316 stainless steel fatigued to failure in strain-controlled tests for nominal inelastic strainranges of 0.4 and 4 percent. Figures 1 and 2 are macrophotographs. Figures 3 and 4 provide SEM photomicrographs superimposed upon plots of inelastic strainrange versus cycles to

failure as reported in reference 7.

Generalized observations were that for this material at a strainrange of nominally 4 percent, the cyclic life relationships (fig. 4) for PC, and CC-cycles show no life reduction from the PP-cycle. The introduction of creep in a CP type cycle, however, appreciably affected life at high as well as at the lower strainranges (fig. 3). For nearly identical cyclic lives and at high inelastic strainranges ($\Delta\varepsilon_i = 4\%$), the fractured surfaces for specimens subjected to PP, PC, and CC-cycles are very similar on a macroscopic scale (figs. 2(a), 2(b), and 2(d)) in that striation "crescents" typical of transgranular fracture are evident. In the case of the CP-cycle (fig. 2(c)) the crystalline appearance indicates that intergranular fracture occurred. At higher magnification, however, (figs. 3 and 4) each of the four types of SRP cycle is seen to produce a distinctively different fracture surface. At high or low strainrange and for the range of temperatures investigated, the specific identification of the mode of fracture for each SRP-cycle is presented in the sections which follow.

PP-cycle Fracture

Striations are evident in figure 5 for AISI 304LC stainless steel. Section AA shows "planar" transgranular fracture broad, unified, crack front, about 60 percent of surface area (inset). Initial test cycles resulted in crystallographic slip, with less than one grain depth of slip-plane cracking as in Stage I fatigue (ref. 2). Fracture is transgranular and the fracture surface has striations across the wall thickness (fig. 5). At higher magnification, "early" and "late" striations are shown in figures 6(a) and 6(b). A single "early" striation, 1.2 μm or about 3000 atoms in thickness, is shown in figure 6(c) at a site undamaged by crack-closure. The actual number of striations counted was 147, with "early" striations of 0.63 μm (slip-band width) and with "late" striations of 70 μm width (about 100 slip bands between striations). "Late" striations were delineated by "terraces" of slip-bands (fig. 6(b)). Ductile tearing occurred during cyclic tensile-loading.

A specific feature of PP-cycle type of fracture of both AISI 304LC or AISI 316 stainless steel is early continuity of striations from grain to grain.

Crack propagation rate or the change in striation width per cycle, dc/dn, is plotted versus crack half-length, c/2, in figure 7 at each of four strainrange levels for AISI 316, and in figure 8 at two strainrange levels for AISI 304LC. Crack length, c, is defined as the total depth of cracking. These figures provide the basis for the summation of table II which shows the percent cyclic life for initiation and propagation to two crack depths at strainranges ranging from 0.4 to 8 percent. The crack depths are 125 μm (0.005 in.) and 375 μm (0.015 in. or 25% of the original wall thickness of the tubular specimens). The plots reveal that striations across the wall thickness can account for from 10 to 100 percent of PP-cyclic life for the strainranges evaluated. Table II shows that where a depth of 125 μm (0.005 in.) is selected as being the depth of a surface detectable crack, then for an inelastic

strainrange of about 0.4 percent, about 80 percent of the PP-cyclic life is expended a crack "initiation". At higher strainranges of 3 to 8 percent, the 125 μm depth is reached in approximately 40 percent of the cyclic life.

In summation, for the two steels examined and for the test conditions evaluated, the characteristics of PP cyclic fracture are:

(1) Transgranular fracture with few initiation sites.

(2) Striations and slip-bands between striations are planar.

(3) Generally, a broad, unified, crack front.

(4) About 80 percent of PP-cyclic life is expended to produce a crack depth of 125 μm at low strainrange, with a decrease to about 40 percent of total cyclic life at the higher strainranges (3 to 8%).

(5) The identifying features were similar over the range of strainrange and temperature applied.

PC-cycle Fracture

Transgranular cracking with slip-bands and many discontinuous crack-fronts are characteristic of PC-cycle type fracture as shown in figure 4. Surface distortion and slip-band cracking probably resulted from grain distortion caused by grain boundary sliding during compressive creep strain. The crack-front is blunted and diverted by the grain boundaries. Cracking initiated at many sites distributed both longitudinally and circumferentially (figs. 1(b) and 2(b)). Crack propagation proceeded transgranularly and grain deformation and multiple crack initiation resulted in delineation of grains on an otherwise planar surface (figs. 1(b) and 2(b)). At higher magnification (fig. 4) continuity of striations across grain boundaries is evident.

Plots (figs. 8 and 9) show a stepwise crack propagation rate. The steps are believed to be the result of multiple cracking which caused the crack front to catch-up or lag-behind the radial path selected for making these plots. From table II it is seen that for both high or low strainranges to reach the 125 μm crack depth, the percent of cyclic life expended is about the same as for the PP-cycle. Some features of PC-cycle fracture are that it generally initiates in fewer cycles than the PP-cycle and at a greater number of sites. The slip-bands, possibly caused by unidirectional slip in each cycle, are broader than those produced by reversed slip in each cycle (as in the PP-cycle). The PC shear-lip is up to 50 percent of the wall thickness, and is circumferential.

In summation, the PC-cycle type of fracture is characterized by the following features:

(1) Planar Transgranular fracture with striations.

(2) Multiple transverse crack initiation sites distributed about the circumference.

(3) Distorted specimen surface and blunted crack fronts diverted at grain boundaries.

(4) Deep shear lip, up to 50 percent of the wall thickness.

(5) The percent of cyclic life expended for crack initiation is about equivalent to that for a PP-cycle.

(6) The PC-cycle has fewer cycles of initiation and shorter cyclic

life than does the PP-cycle at an equivalent inelastic strainrange.

(7) The identifying features were similar over the range of strainrange and temperature applied.

CP-cycle Fracture

All CP-cycle specimen failures are characterized by intergranular fracture (figs. 1,2,3,10, 11, and 12). Internal cracking was observed. Cracking throughout the cross-section is by grain boundary fracture. Cracking in those grain boundaries perpendicular to the stress axis is by cleavage. Cracking in those boundaries which are not cleaved is characterized by terrace markings or "strians" ((figs. 10(a) and 10(b)). Because of internal crack initiation at multiple internal sites, a direct determination of crack propagation cycles was not possible. For the CP-cycle, specimen failure occurred at a total cyclic life less than that required for crack initiation for the PP, PC, and CC-cycles.

From the plots of strainrange versus cycles to failure (figs. 3 and 4), the CP intergranular fracture mode is seen to be the most damaging. At high strainrange, in particular, the CP-cycle type of fracture is closest in appearance to that of monotonic creep fracture. That is, the fracture surfaces are faceted where grain boundaries have separated (fig. 12(a)). Unlike monotonic creep rupture which involves simple grain separation and ductile elongation of material between grain fractures, the separation of grains in the CP-cycle occurred by a slip-band producing mechanism suggestive of the striations produced by transgranular fatigue crack propagation. The cyclic fatigue character of the CP-cycle intergranular fracture is revealed by grain boundary slip-bands and groupings of slip-bands. These might expected to form for each cycle of crack propagation from the internal initiation sites very much as striations are formed from external initiation sites. These features which distinguish intergranular fatigue cracking from intergranular monotonic fracture are designated "strians", herein. "Strians," it is suggested, are intergranular markings which are related to cycles of crack growth in much the same way as are striations which appear across grains where cracking is transgranular in nature. Metallographic and schematic examples of "strian"-formation are shown in figures 10 and 11. By making a sample count of "strians" per unit length of test specimen wall thickness on several CP-cycle fractured surfaces (at 300X to 1000X using the SEM), the number of "strians" increased with increased cycles-to-failure. Thus, a qualitative association was made between "strian"-count and cycles of crack propagation.

In summation, the characteristics of CP-cycle type of fracture were found to be as follows:

(1) Intergranular fracture at multiple internal sites.

(2) Grain-boundary "strian" markings.

(3) Cracking of grain boundaries normal to stress-direction, with propagation by slip-band fracture at tilted grain boundaries.

(4) For any inelastic strainrange from 0.4 to 4 percent, test specimens subjected to the CP-cycle failed in fewer cycles than are required for formation of a 125 μm deep crack under conditions of PP,

PC, and CC cycling.

(5) The identifying features were similar over the range of strainrange and temperature applied.

CC-cycle Fracture

Semi-planar mixed fracture cracking, and dislocated surface grains are evident in figures 4 and 12(b). CC-cycle fracture is characterized by intergranular cracking in addition to transgranular propagation, discontinuous from grain to grain.

For AISI 316, at two levels of strainrange, the generally planar, mixed-fracture, appearance is evident in figures 1(d) and 2(d). A crescent-shaped crack front is evident in figure 1(d). The fracture has a distinctive semi-planar granular topography which is particularly evident in figures 2(d) and 12(b). The intergranular character of CC-cyclic fracture appears to be introduced by reversed creep strain as the crack front advances. The CC-cycle crack-propagation plot (fig. 13) was based on an average of measurements taken along several radial intercepts because of distortion and differing slip-band width in adjacent grains. Since a lesser percent of total cyclic life (about 35% to 45% at 4% to 0.4% strainrange, table II) was expended for CC-cycled specimens to initiate a crack 125 μm deep than for the PP or PC cycles, it might be expected that the CC-cycle would have the shortest total cyclic life of these three SRP-cycles. This is true, however, only at lower strainranges. At 4.0 percent inelastic strainrange, the lives of CC, PC, and PP-cycled specimens are about the same. The damaging aspect of the CC-cycle as compared to the PC and PP-cycle is the tensile creep component which produces early crack initiation to a depth of 125 μm. At inelastic strainranges below about 1 percent, a further contribution to damage may be associated with crack propagation-to-failure. It appears that intergranular cracking occurred in addition to transgranular cracking, most probably, at the crack front as it advanced. Compared to CP-cyclic life at any inelastic strainrange, it should be noted (fig. 4) that tensile creep (as in the CP-cycle) is an order of magnitude more damaging than tensile creep which is offset by compressive creep (as in CC). For either the CC or CP cycles it is probably tensile creep which produces the damaging intergranular cracking.

In summation, the CC-cycle resulted in cracking which progressed by mixed transgranular and intergranular fracture modes, such that CC-cycle fracture is characterized by:

(1) Semi-planar mixed fracture.

(2) Grain-deformation which resulted in grain boundary cracking the fracture plane.

(3) Crescent-shaped, but irregular, crack-propagation front.

(4) About 35 to 45 percent of total cyclic life is expended to reach a 125 μm depth over the range of inelastic strainranges evaluated.

(5) The identifying features were similar over the range of strainrange and temperature applied.

CONCLUDING REMARKS

The results of this study supplement metallurgical data previously reported for several materials which showed similar fracture and strainrange/cyclic life behavior; for example, the Fe-base alloy A286 (ref. 5) and the Ta alloy T111 (ref. 6). For these materials the SRP lines are separated and the fracture appearance differed for each type of SRP cycle evaluated. The inference that may be drawn from all of this work is that creep and the direction of creep strongly influences both the fracture mechanism and the cyclic life.

Grain-boundary fracture surface markings, designated "strians," are proposed as a means of identifying CP-cycle intergranular crack growth cycles. This may be possible much in the same way that "striation-count" is related to cycles of crack growth for transgranular cracking.

SUMMARY OF RESULTS

The following major results were obtained from an investigation to characterize the HTLC creep fatigue cracking of AISI 304LC and 316 stainless steel specimens for each of four basic inelastic strain relationships obtained by the method of Strainrange Partitioning:

1. Each of the four basic inelastic-strain Strainrange Partitioning (SRP) cyclic fatigue-life relationships were found to result in a distinctively characteristic fracture mode over the range of strainranges (0.4% to 4%) and temperatures (305°C to 705°C) evaluated. It was generally noted that the SRP fracture modes, as had previously been shown for the SRP-cyclic-life relationships, were relatively temperature independent.

2. The PP-cycle, with transgranular cracking, had few crack initiation sites. Striations were planar with slip-bands between striation marks.

3. Compressive creep strain (PC-cycle) acted to cause multiple initiation sites and early onset of transgranular cracking. There were fewer cycles for crack initiation and a shorter cyclic life for an equivalent inelastic strainrange as compared to the PP-cycle.

4. Reversed-creep strain (CC-cycle) acted to advance the crack-front by grain boundary fracture combined with transgranular propagation.

5. Tensile-creep strain (CP-cycle) imposed damage by grain boundary cracking throughout the section thickness. The CP-cycle type of fractures were intergranular at all strainrange levels investigated.

6. Fracture of the CP-cycled specimens occurred in fewer cycles than were required for specimens subjected to other types of SRP-cycles to develop a crack 125 μm deep.

REFERENCES

1. Manson, S. S.: The Challenge to Unify Treatment of High Temperature Fatigue - a Partisan Proposal Based on Strainrange Partitioning. Fatigue at Elevated Temperatures, Am. Soc. Test. Matls. Spec. Tech. Publ.-520, 1973, pp. 744-782.

2. Manson, S. S.; Halford, G. R.; and Nachtigall, A. C.: Separation of the Strain Components for Use in Strainrange Partitioning. Advances in Design for Elevated Temperature Environment, ASME, 1975, pp. 17-28.

3. Forsyth, P. J. E.: Fatigue Damage and Crack Growth in Aluminum Alloys. Acta. Met., vol. 11, no. 7, July, 1963, pp. 703-715.

4. Wood, W. A.; Cousland, S. McK.; and Sargant, K. R.: Systematic Microstructural Changes Peculiar to Fatigue Deformation. Acta. Met. vol. 11, no. 7, July, 1963, pp. 643-652.

5. Manson, S. S.: Interfaces Between Fatigue, Creep, and Fracture. Int. J. Fract. Mech., vol. 2, no. 1, Mar. 1966, pp. 327-363.

6. Sheffler, K. D.; and Doble, G. S.: Influence of Creep Damage on the Low-cycle Thermal-Mechanical Fatigue Behavior of Two Tantalum-Base Alloys. (TRW-ER-7592, TRW Equipment Labs.; NASA Contract NAS3-13228.) Also, Fatigue at Elevated Temperatures Am. Soc. Test. Matls. Spec. Tech. Publ.-520, 1973, pp. 491-499.

7. Hirschberg, M. H.; and Halford, G. R.: Use of Strainrange Partitioning to Predict High Temperature Low-cycle Fatigue Life. NASA TN D-8072, 1976.

8. Hirschberg, M. H.: A Low Cycle Fatigue Testing Facility. Manual on Low Cycle Fatigue Testing, Am. Soc. Test. Matls. Spec. Tech. Publ. 465, 1970, pp. 67-86.

TABLE I. - TEST SPECIMEN HISTORY AND PREPARATION FOR FIGURES

Figure	Specimen number	SRP-cycle P = plastic flow C = creep	Strainrange $\Delta\varepsilon_i/\Delta\varepsilon$ %	Temperature tension/comp °C	Cycles to fail	SEM[1] fracture surface	
						Preparation[1]	Magnification
	316 Stainless steel						
1(a)	211	PP	0.4/0.4	705	11 980	None[1]	13X
1(b)	169	PC	1.3/0.6	↓	345	↓	↓
1(c)	159	CP	0.5/0.4		275		
1(d)	136	CC	0.44/0.34		1150		
2(a)	132	PP	3.5/3.5	705	102	None[1]	13X
2(b)	100	PC	3.6/2.5	↓	88	↓	↓
2(c)	160	CP	3.7/2.5		12		
2(d)	129	CC	3.8/3.3		98		
3	240	CP	2.0/1.2	650/315	22	None[1]	300X
↓	132	PP	3.5/3.5	705	102	↓	↓
	218	CP	0.19/0.12	815	3090		
	95	PP	0.4/0.4	705	1700		
4	129	CC	3.7/3.3	705	98	None[1]	300X
↓	100	PC	3.6/2.5	705	88	↓	↓
	136	CC	0.44/0.34	705	1150		
	205	PC	0.9/0.65	315/705	811		
7	328	PP	8.0	650	5	None[1]	Crack growth plots (determined at 300X to 10 000X)
↓	325	↓	3.0	650	60	↓	
	95		.42	705	1700		
	211		.38	315	11 980		
9	100	PC	3.6/2.5	705	88		
9	205	PC	0.9/0.7	315/705	811		
10(a)	159	CP	0.5/0.4	705	275	As etched[3]	300X
10(b)	159	CP	0.5/0.4	705	275	None[1]	300X
13	129	CC	3.8	705	98	None[1]	Crack-growth plots
13	136	CC	0.44/0.34	705	1150	None[1]	
	304 Stainless steel						
5	51	PP	1.8/1.8	593	166	Au[2]-coated (SEM)	3X,100X,[2]150X[3]
6	51	PP	1.8/1.8	593	166	Au[2]-coated (SEM)	1000X, 30 000X
8	53	PC	2.7/1.8	565	200	None[1]	Crack growth plots
8	51	PP	1.8/1.8	593	166	Au-coated (SEM)	Crack growth plots
12(a)	39	CP	3.6/3.0	650	9	None	300X
12(b)	61	CC	2.2/1.9	650	88	None	300X

[1] No oxide removal was used. Specimens ultrasonically cleaned in freon PCA for scanning electron microprobe (SEM).

[2] Vapor-deposition of gold to prevent charging effects, author prefers only at high mag.

[3] Metallographic section, axial (mounted in plastic bias); H_2O + 20% Oxalic, electrolytic etch.

TABLE II. - PERCENT CYCLIC LIFE FOR FORMATION OF CRACKS OF TWO SPECIFIC DEPTHS

Loading cycle	Strainrange, %	% Life to crack depth*	
		5 mils, 125 μm	15 mils, 375 μm
316 Stainless steel			
PP	0.4	79, 83	90, 86
	3.0	42	86
	8.0	40	100
PC	0.9	77	86
	3.6	40	57
CC	0.4	45	86
	3.8	34	68
304 Stainless steel			
PP	1.8	75	89
PC	2.7	91	99

*Based on total cyclic life minus the number of striations as a percent of life.

(a) PP-cycle, $\Delta\varepsilon_i$ = 0.4%;
(11 980~), $\Delta\varepsilon_{pp}$ = 0.4%.

(b) PC-cycle, $\Delta\varepsilon_i$ = 1.3%;
(345~), $\Delta\varepsilon_{pc}$ = 0.6%.

(c) CP-cycle, $\Delta\varepsilon_i$ = 0.5%;
(275~), $\Delta\varepsilon_{cp}$ = 0.4%.

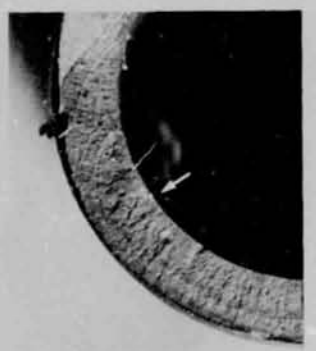

(d) CC-cycle, $\Delta\varepsilon_i$ = 0.4%;
(1150~), $\Delta\varepsilon_{cc}$ = 0.3%.

Figure 1. - Low strainranges (0.4 to 0.9%), HTLCF produce characteristic fractures as shown (705° C). Final fracture is at upper left-hand corners. AISI 316 stainless. X13.

(a) PP-cycle, $\Delta\varepsilon_i$ = 3.5%;
(102~), $\Delta\varepsilon_{pp}$ = 3.5%.

(b) PC-cycle, $\Delta\varepsilon_i$ = 3.6%;
(88~), $\Delta\varepsilon_{pc}$ = 2.5%.

(c) CP-cycle, $\Delta\varepsilon_i$ = 3.7%;
(12~), $\Delta\varepsilon_{cp}$ = 2.5%.

(d) CC-cycle, $\Delta\varepsilon_i$ = 3.8%;
(98~), $\Delta\varepsilon_{cc}$ = 3.3%.

Figure 2. - High strainranges (3.5 to 3.8%) HTLCF produce fractures with features accentuated but similar to characteristic low strainrange HTLCF fracture, figure 1. AISI 316 stainless, 705° C. X13.

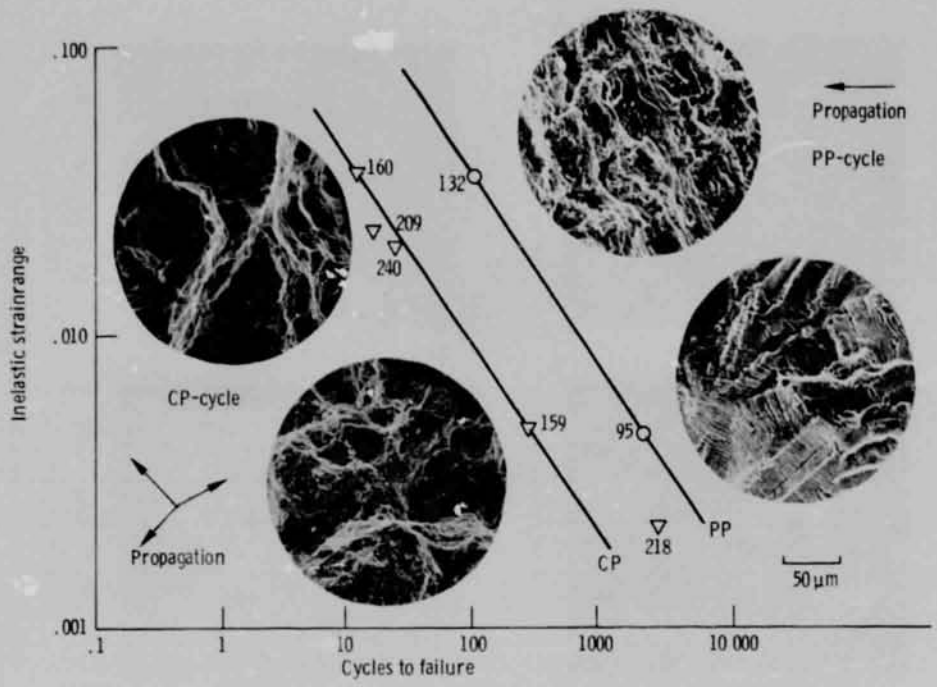

Figure 3. - Strainrange vs cyclic-life and fractographs showing creep predominate in intergranular fracture with terraced grain boundary "strians" of CP-cycle (left) and striations formed by crack front of PP-cycle (right).

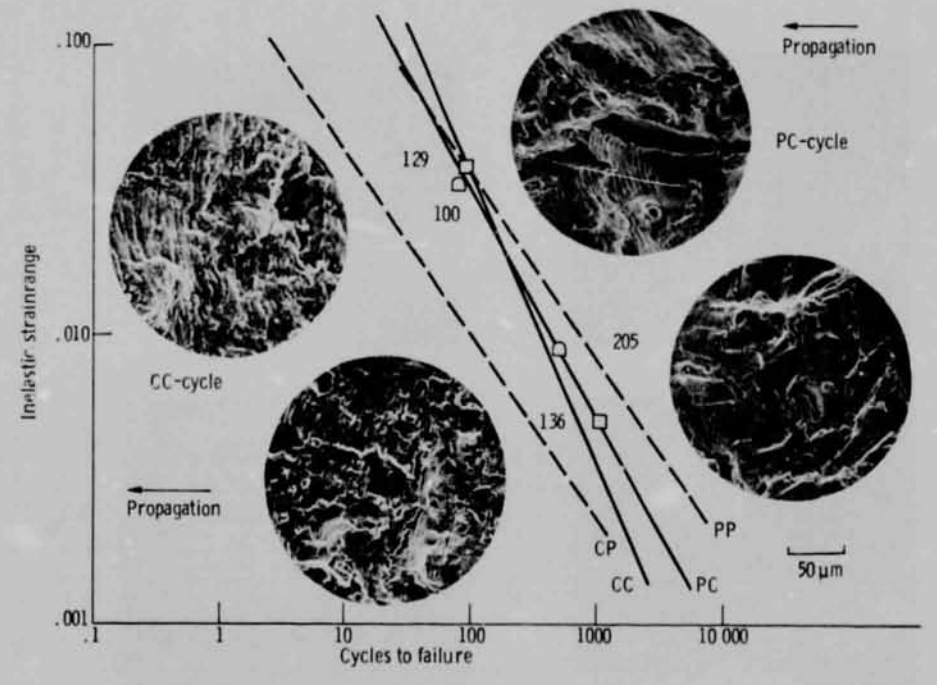

Figure 4. - Strainrange vs cyclic-life and fractographs showing planar mixed-fracture advance of crack with compressive creep (CC-cycle), left and planar distorted-striations of tensile creep (PC-cycle), right. AISI 316 stainless steel.

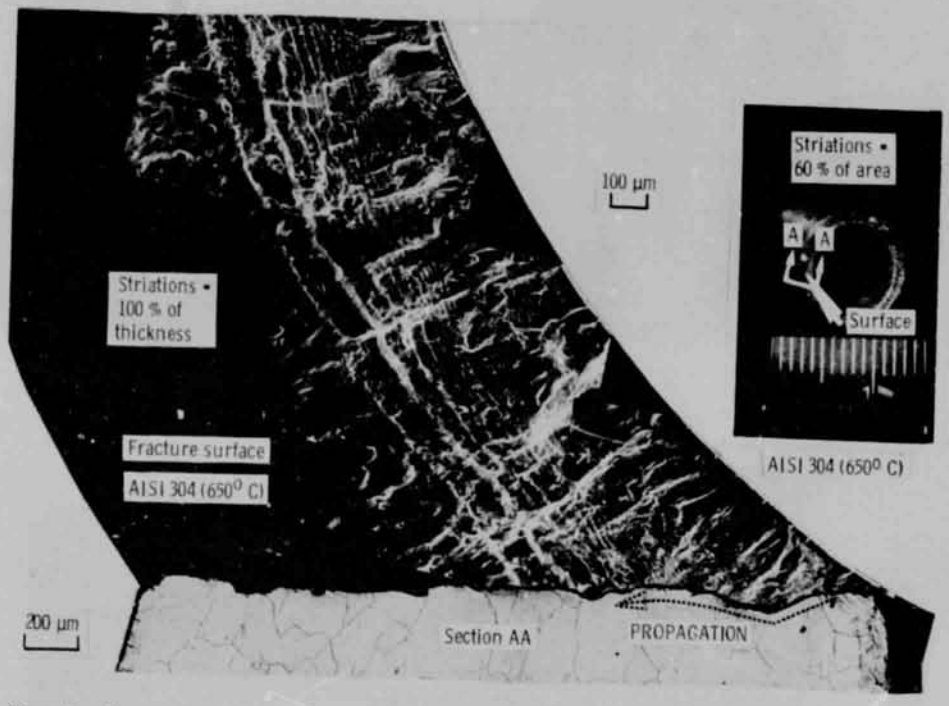

Figure 5. - Planar, striation-fracture surface and metallographic section for PP-cycled AISI 304 stainless steel, 650° C, X100. Etchant (section): H_2O + 20 % oxalic (electrolytic).

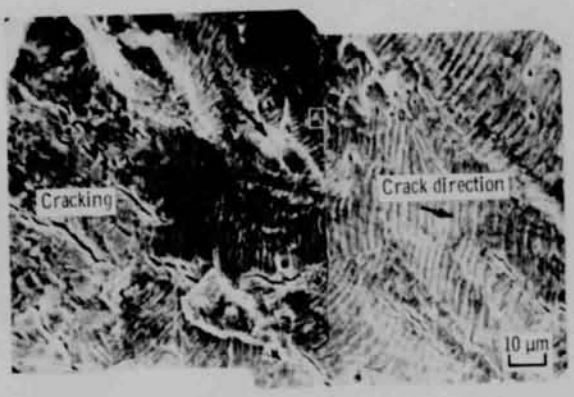

(a) 'Early' striations (block is (c)).

(c) Single striation.

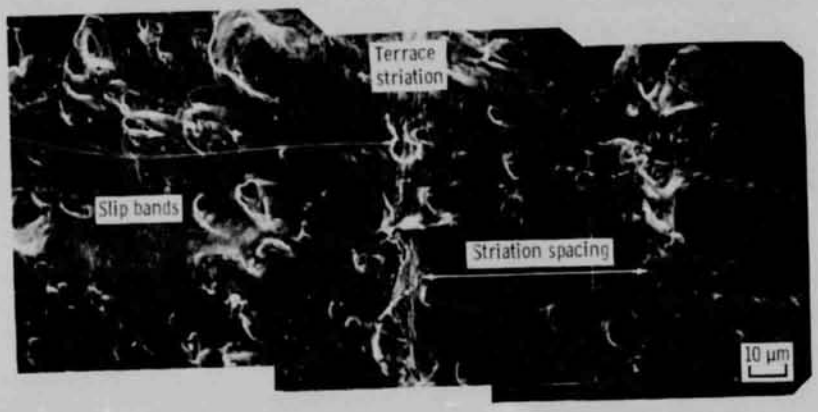

(b) 'Late' striations; $\Delta\varepsilon_i$ = 1.76%, $\Delta\varepsilon_{pp}$ = 1.76% (166 cycles).

Figure 6. - Striation details for PP-cycled AISI 304 (650° C). Fracture surface plastic-plastic fatigue-cycled specimen.

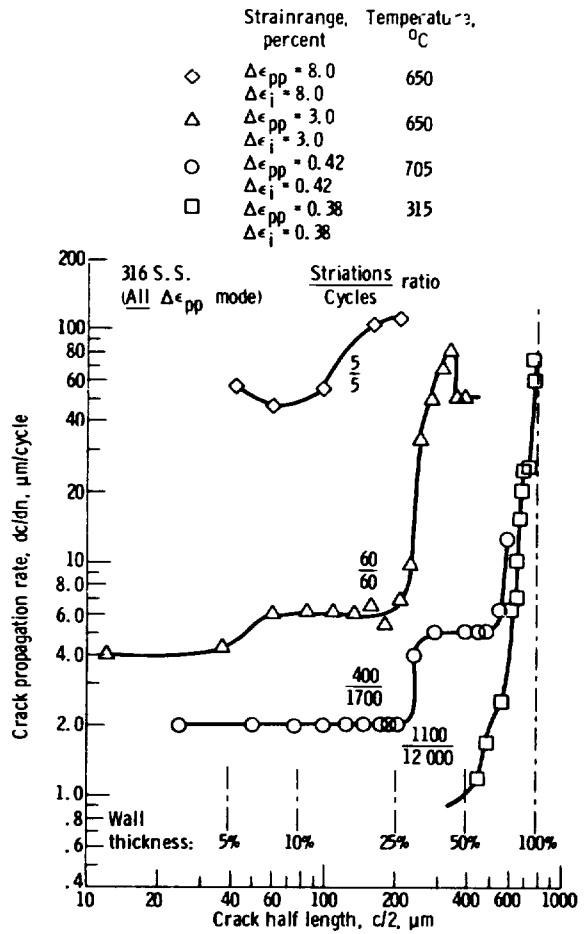

Figure 7. - Effect of strainrange on crack propagation rate as a function of crack depth. Ratios (rounded) indicate the fraction of cyclic life evidenced by striations. PP-cycle, 316 S.S.

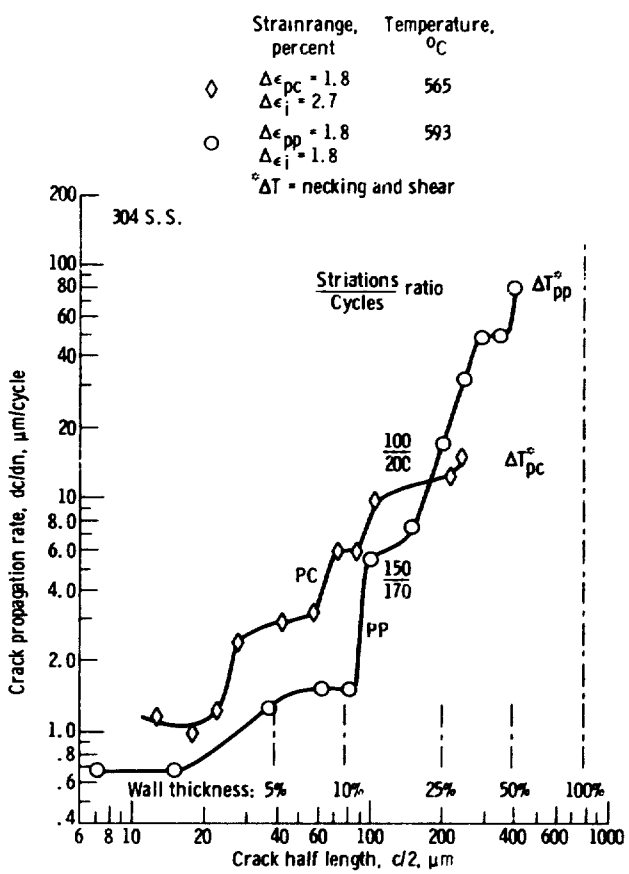

Figure 8. - Comparison of crack propagation rate as a function of crack depth for PP- and PC-cyclic loading. Ratios (rounded) indicate the fraction of cyclic life evidenced by striations. 304LC S.S.

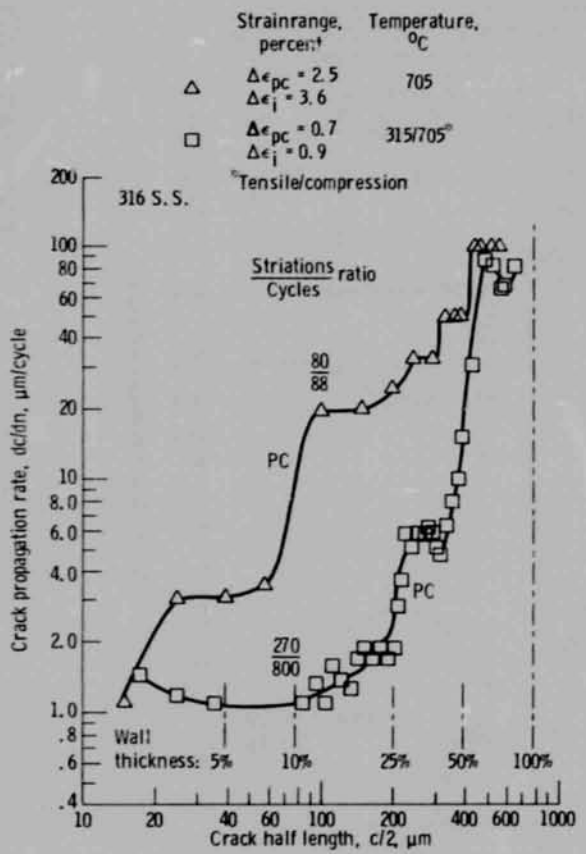

Figure 9. - Effect of strainrange on crack propagation rate as a function of crack depth. Ratios (rounded) indicate the fraction of cyclic life evidenced by striations. PC-cycle, 316 S.S.

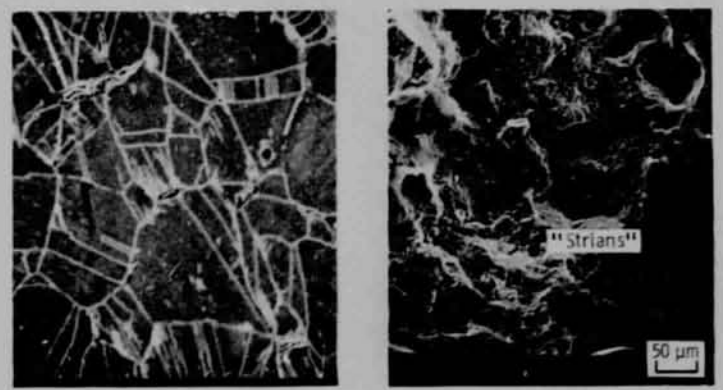

(a) Internal cracking by fracture of grain boundaries and localized slip.

(b) Fracture surface showing grain-boundary cleavage-facets perpendicular to load-axis and "strians" on shear-planes between grains.

Figure 10. - Internal grain boundary cracking in a metallurgical section and "strian" formation on the fracture surface of a CP-cycled test specimen. AISI 316 stainless steel. X300.

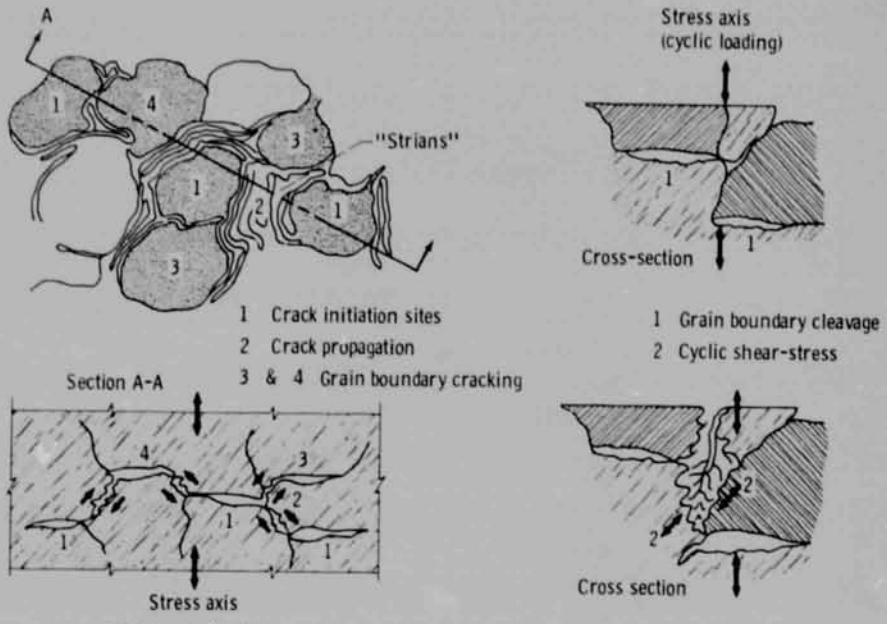

(a) CP-cycle fracture.

(b) Crack propagation along grain boundaries.

Figure 11. - Schematic formation of "terraced" grain boundaries, 2 , designated "strians." CP-cycle intergranular fracture.

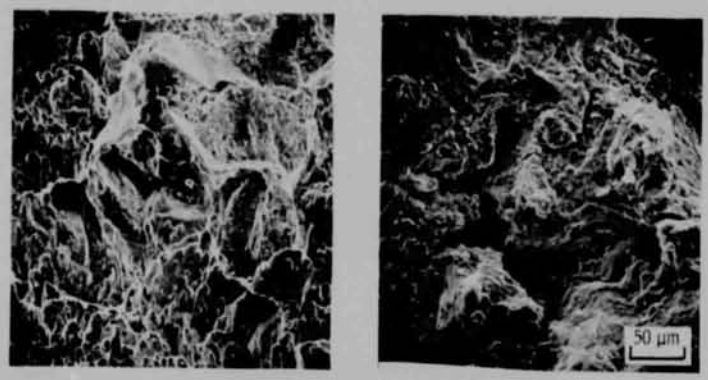

(a) $\Delta\varepsilon_{cp}$ = 3.02% (9 cycles); $\Delta\varepsilon_i$ = 3.55%.

(b) $\Delta\varepsilon_{cc}$ = 1.88% (88 cycles); $\Delta\varepsilon_i$ = 2.16%.

Figure 12. - Fracture characteristics of tensile creep (CP-cycle) and fully-reversed creep (CC-cycle) HTLCF of AISI 304 (650° C) SEM. X300.

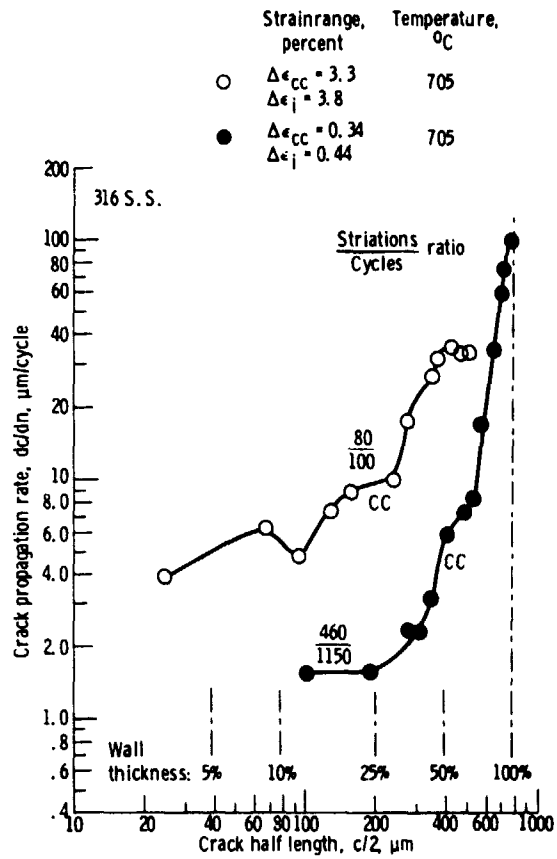

Figure 13. - Effect of strainrange on crack propagation rate as a function of crack depth. Ratios (rounded) indicate the fraction of cyclic life evidenced by striations. CC-cycle, 316 S.S.

1 Report No	2 Government Accession No.	3 Recipient's Catalog No
NASA TM-78913		

4 Title and Subtitle	5 Report Date
FRACTOGRAPHIC EVALUATION OF CREEP EFFECTS ON STRAIN-CONTROLLED FATIGUE-CRACKING OF AISI 304LC AND 316 STAINLESS STEEL	June 1978
	6. Performing Organization Code
7 Author(s)	8 Performing Organization Report No
Robert E. Oldrieve	E-9648
	10. Work Unit No
9 Performing Organization Name and Address	
National Aeronautics and Space Administration Lewis Research Center Cleveland, Ohio 44135	11. Contract or Grant No.
	13 Type of Report and Period Covered
12. Sponsoring Agency Name and Address	Technical Memorandum
National Aeronautics and Space Administration Washington, D.C. 20546	14. Sponsoring Agency Code

15. Supplementary Notes

16 Abstract

Analysis of high temperature low cycle fatigue of AISI 304LC and 316 stainless steels by the method of strainrange partitioning results in four separate strainrange versus life relationships, depending upon the way in which creep-strain and plastic strain are combined within a cycle. Fractography is used in this investigation of the creep-fatigue interaction associated with these cycles. The PP and PC-cycle fractures were transgranular. The PC-cycle resulted in fewer cycles of initiation and shorter total cyclic life for the same applied inelastic strainrange. The CC-cycle had mixed transgranular and intergranular fracture, fewer cycles of initiation and shorter cyclic life than PP or PC. The CP-cycle had fully intergranular cracking, and failed in fewer cycles than were required for cracks to initiate for PP, PC, and CC.

17. Key Words (Suggested by Author(s))	18. Distribution Statement
Fatigue; Materials; Metallography; Stainless steels; Structures; Fracture mechanisms; Structural materials	Unclassified - unlimited STAR Category 39

19. Security Classif (of this report)	20. Security Classif (of this page)	21. No. of Pages	22 Price*
Unclassified	Unclassified		

* For sale by the National Technical Information Service, Springfield, Virginia 22161